Journal of the Physical Society of Japan
Vol. 78, No. 1, January, 2009, 013702

Thermoelectric and Magnetic Properties of a Narrow-Gap Semiconductor $FeGa_3$

Yuta HADANO[1], Shouta NARAZU[1], Marcos A. AVILA[1], Takahiro ONIMARU[1], and Toshiro TAKABATAKE[1,2*]

[1]*Department of Quantum Matter, ADSM, Hiroshima University, Higashihiroshima, Hiroshima 739-8530*
[2]*Institute for Advanced Materials Research, Hiroshima University, Higashihiroshima, Hiroshima 739-8530*

(Received October 23, 2008; accepted November 4, 2008; published December 25, 2008)

We report transport, thermal, and magnetic measurements on single crystalline samples of $FeGa_3$ prepared by a Ga self flux method. The electrical resistivity and Hall coefficient at temperatures above 300 K display semiconducting behaviors with energy gaps of 0.47 and 0.54 eV, respectively, whose values agree with the calculated band gap. In the saturation range 100–260 K, the carrier mobility μ exhibits an unusual dependence on temperature; $\mu(T) \propto T^{-5/2}$. The thermopower has a large negative minimum of $-350\,\mu V/K$ at 300 K. The diamagnetic susceptibility weakly depends on temperature, which confirms the absence of localized magnetic moments. The T-linear coefficient of the specific heat is $0.03\,mJ/(K^2 \cdot mol)$, being two orders of magnitude smaller than that reported for Fe-based Kondo semiconductors FeSi and $FeSb_2$.

KEYWORDS: $FeGa_3$, narrow-gap semiconductor, Kondo semiconductor, thermoelectric properties, magnetic susceptibility
DOI: 10.1143/JPSJ.78.013702

Intermetallic compounds based on $3d$ and $4d$ transition elements are usually metallic. However, there is a class of semiconductors such as $RuAl_2$,[1] Fe_2VAl,[2] FeSi,[3–9] and $FeSb_2$,[10–14] in which a gap of the order of 0.1 eV is produced by the hybridization of transition metal d states with p states of group 13 and 14 elements. These narrow-gap semiconductors have high thermopower, which is the most important requisite for thermoelectric application. The thermoelectric efficiency is evaluated by the figure of merit $Z = S^2/\rho\kappa$, where S is the thermopower, ρ is the electrical resistivity, and κ is the thermal conductivity. Among above mentioned compounds, $FeSb_2$ exhibits the largest thermopower of $-45000\,\mu V/K$ at 10 K,[14] which in turn gives rise to the extremely high power factor S^2/ρ being 65 times larger than that of the conventional Bi_2Te_3-based materials. Both FeSi[3–9] and $FeSb_2$[10–14] have attracted much attention not only due to the feasibility of thermoelectric materials but also due to strongly correlated electron properties similar to rare-earth-based Kondo semiconductors. The hallmark of a Kondo semiconductor is that the gap disappears at a temperature which is low relative to the gap energy. Such a characteristic feature was observed for FeSi and $FeSb_2$ by the temperature dependent optical conductivity measurements.[4,12] Typical Kondo semiconductors YbB_{12} and $Ce_3Pt_3Bi_4$ have a gap of 0.02 eV, whose value is one order of magnitude smaller than in the above mentioned $3d$ compounds. The gap opens in a renormalized band which is formed by the hybridization of rather localized $4f$ states with the conduction bands.[15]

The iron-based compound $FeGa_3$ crystallizes in a tetragonal structure with the space group $P4_2/mnm$.[16] The band structure calculations based on the density-functional theory within the local density approximation led to a d(Fe)–p(Ga) hybridization gap of 0.3–0.5 eV.[17,18] The valence band maximum occurs at A and the conduction band minimum occurs at a point between Z and Γ. The presence of a gap smaller than 0.8 eV was indicated by a valence-band x-ray photoemission measurement at 55 K.[19] However, an activation type behavior in $\rho(T)$ with a small gap energy $E_g = 240$ K was observed at temperatures only below 100 K even for a single crystal, and the presence of a minimum in $\rho(T)$ at 160 K was considered to contradict with the calculated band gap.[17] The magnetic susceptibility $\chi(T)$ of $FeGa_3$ was found to be negative (-4×10^{-5} emu/mol) at 300 K. It becomes positive above 720 K and increases to 2×10^{-5} emu/mol on heating to 800 K.[19] This temperature dependence resembles that of FeSi and $FeSb_2$,[3,5,11] whose $\chi(T)$ data were explained using a model of two narrow bands separated by 940 and 870 K, respectively.[5,11] The application of this model to $\chi(T)$ data for $FeGa_3$ led to a larger gap of 5200 K.[19]

The thermoelectric figure of merit of $FeGa_3$ polycrystalline samples has been assessed by measurements of thermoelectric properties at high temperatures, 300–1000 K.[20] The $S(T)$ has a large negative value of $-500\,\mu V/K$ at 313 K and approaches $-50\,\mu V/K$ on heating to 950 K. The n-type carrier density at 300 K was estimated to be $3 \times 10^{18}/cm^3$, whose value falls in the range for good thermoelectric materials. However, because of the low mobility of carriers, the value of $\rho = 200\,m\Omega\,cm$ at 300 K is two orders of magnitude larger than that of the conventional thermoelectric material Bi–Te.[21] Therefore, the maximum ZT value resulted at a rather low level of 0.04 at 973 K.

In this work, we aimed to study to what extent the nature of Kondo semiconductor resides in $FeGa_3$. For this purpose, it is necessary to measure magnetic and transport properties of well-characterized single crystals at low temperatures. With this in mind, we have grown single crystals of high purity and measured the χ, ρ, S, κ, Hall coefficient R_H, and specific heat C at temperatures down to 4 K. Here, we present the experimental results and discuss them in comparison to those of Kondo semiconductors FeSi and $FeSb_2$.

Single crystals of $FeGa_3$ were grown by a Ga self-flux method. A mixture of high purity Fe and Ga in a composition of 1 : 9 was sealed in an evacuated silica

*E-mail: takaba@hiroshima-u.ac.jp

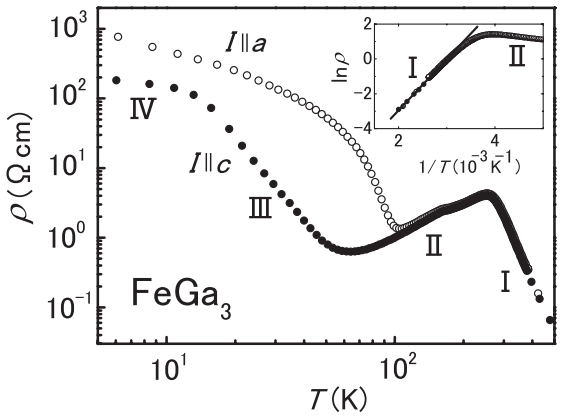

Fig. 1. Temperature dependence of electrical resistivity $\rho(T)$ of $FeGa_3$ for the current directions along the tetragonal a- and c-axes. The inset shows $\ln\rho$ vs T^{-1} in the temperature range 300–500 K. A fit with the Arrhenius law $\rho(T) = \rho_0 \exp(E_g/2k_BT)$ gives the energy gap $E_g = 0.47$ eV.

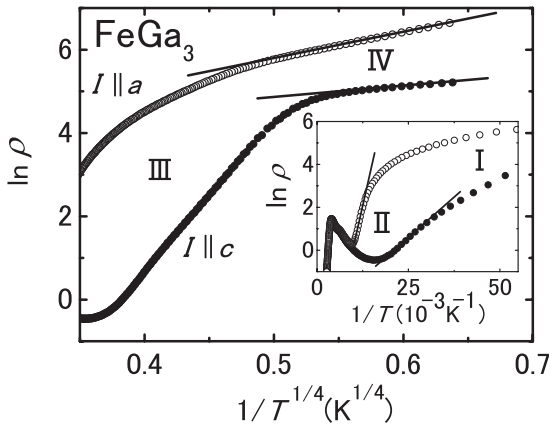

Fig. 2. Temperature dependence of the electrical resistivity $\rho(T)$ of $FeGa_3$ in the form of $\ln\rho$ vs $T^{-1/4}$ which is fitted by the hopping conduction's expression $\rho(T) = \rho_0 \exp[(T_0/T)^{1/4}]$ with $T_0(I \| a) = 1700$ K and $T_0(I \| c) = 77$ K. The inset shows $\ln\rho$ vs T^{-1} in the temperature range 20–100 K. The fit by the expression $\rho(T) = \rho_0 \exp(E_D/2k_BT)$ gives the donor binding energies $E_D = 0.13$ and 0.018 eV for $I \| a$ and $I \| c$, respectively.

ampoule. The ampoule was heated to 1100 °C and cooled to 400 °C for 150 h, where the molten Ga flux was separated by decanting. The obtained single crystals were approximately 10 mm in diameter. The x-ray diffraction analysis on a powdered sample showed a single phase of the $FeGa_3$-type structure. The lattice parameters $a = 6.262$ and $c = 6.556$ Å are in good agreement with reported values.[17] The good stoichiometry was confirmed by electron-probe microanalysis using a wavelength dispersive JEOL JXA-8200 system. The inclusion of Ga flux was found to be less than 3%.

The measurements of ρ were performed using home-built systems with a standard four-probe method in two ranges 3–380 and 300–500 K. In the former range, a Gifford–McMahon type refrigerator was used, while in the latter a vacuum chamber with a resistance heater was used. The R_H was measured by an AC method in the temperature range 100–370 K by reversing the direction of a magnetic field of 0.1 T. The S was measured in the temperature ranges 4.2–300 and 300–700 K, respectively, using a home-made setup with a differential method and a commercial MMR Seebeck effect measurement system. The κ was measured by a steady-heat-flow method from 4.2 to 300 K. The measurement of C from 2 to 300 K was carried out by a relaxation method (Quantum Design PPMS). The magnetization M was measured with the use of a SQUID magnetometer (Quantum Design MPMS) from 2 to 300 K.

Figure 1 shows $\rho(T)$ of $FeGa_3$ single crystals for electrical current directions $I \| a$ and $I \| c$. The presence of a minimum in $\rho(T)$ at 50–100 K agrees with the result reported on a single crystalline sample.[17] We notice four temperature ranges, I; above 260 K, II; between 260 and 100 K (60 K) for $\| a$ ($\| c$), and III; between 100 K (60 K) and 20 K (16 K), and IV; below 20 K (16 K). The data in range I are plotted as $\ln\rho$ vs $1/T$ in the inset of Fig. 1. The fit with the Arrhenius law, $\rho/\rho_0 = \exp(E_g/2k_BT)$, gives E_g of 0.47 eV for both $I \| a$ and $I \| c$. Since this value agrees with $E_g = 0.3$–0.5 eV obtained from band structure calculations,[17,18] range I is likely determined by the intrinsic response of this compound. In contrast, $\rho(T)$ decreases on cooling from 260 to 100 K (60 K), so range II is thus identified as the saturation range where all of the impurity donors are thermally activated. In range III, we find again an activation behavior as shown in inset of Fig. 2. This is considered as an extrinsic range, where the impurity donors freeze out. In fact, some sample dependence was observed in $\rho(T)$ in this range. The slope of the Arrhenius plot in the inset of Fig. 2 gives donor binding energies $E_D = 0.13$ and 0.018 eV for $I \| a$ and $I \| c$, respectively. With further decreasing of temperature below 20 K (16 K), the $\rho(T)$ varies as $\exp[(T_0/T)^{1/4}]$, which is known as a characteristic of the electron conduction due to variable range hopping among the Anderson localized states in a three-dimensional system.[22] The anisotropic behaviors between ρ_a and ρ_c below 100 K may be attributed to an extrinsic impurity band structure with a donor level just below the conduction band. It is noteworthy that the anisotropy in the ranges I and II is very weak in spite of the tetragonal structure.

Figure 3(a) represents the $R_H(T)$ measured in a field of 0.1 T applied along the a- and c-axes. The two sets of data agree well and decrease linearly with decreasing temperature from 300 to 100 K. Assuming a single-band model for electron-like carriers, the temperature dependences of the density n and mobility μ are evaluated as $n = 1/e|R_H|$ and $\mu = |R_H|/\rho$, respectively. As shown in Fig. 3(b), $n(T)$ increases gradually from 100 to 260 K, above which it rapidly increases probably due to the thermal excitation of electrons over the gap to the conduction band. As shown in the inset of Fig. 3(b), fitting of the activation behavior of $n(T)$ gives $E_g = 0.54$ eV, whose value agrees with that estimated from the activation energy in $\rho(T)$. A double logarithmic plot in the inset of Fig. 3(a) reveals that $\mu(T)$ is proportional to $T^{-5/2}$ in range II. The exponent of 5/2 is larger than 3/2 expected for conventional intrinsic semiconductors.[23] The $T^{-5/2}$ behavior was reported in the saturation range of narrow-gap semiconductors such as β-$FeSi_2$[24] and PbTe-based materials.[25] Thereby, the $T^{-5/2}$ dependence was explained by the combination of various carrier scattering mechanisms; acoustic phonons, polar and nonpolar optical phonons, and ionized impurities.[24]

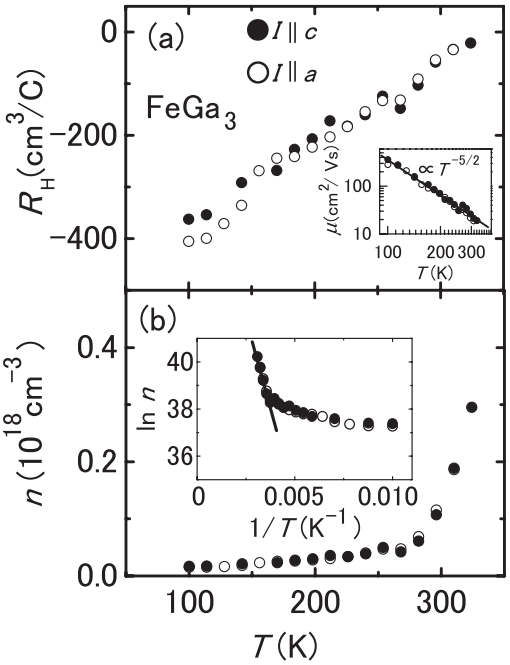

Fig. 3. (a) Temperature dependence of the Hall coefficient R_H for $FeGa_3$. The inset is the double logarithmic plot of the career mobility μ vs temperature. (b) Temperature dependence of the career density n. The inset shows $\ln n$ vs T^{-1}.

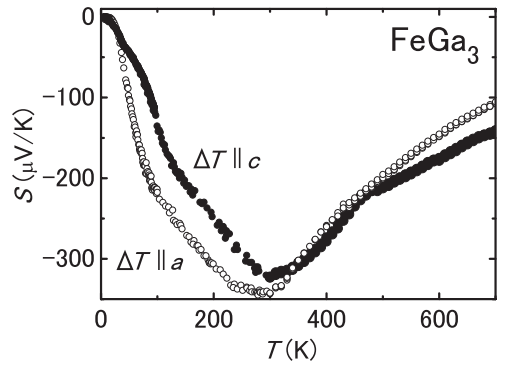

Fig. 4. Temperature dependence of thermopower $S(T)$ for a single crystal of $FeGa_3$ for the temperature gradient along a- and c-axes.

Figure 4 displays $S(T)$ for the temperature gradient directions parallel to the a- and c-axes. The negative sign is consistent with that of $R_H(T)$. After passing through a large minimum of $-350\,\mu V/K$ at 300 K, $|S(T)|$ gradually decreases, which is ascribed to the thermal excitation of electrons above the gap. The large negative $S(T)$ of $FeGa_3$ originates from the enhanced effective mass due to sharp peak of the density of states just above the band gap.[20] The band structure calculations indicated that the curvature of the conduction band bottom is smaller than that of the valence band top.[17,18] This fact implies the larger effective mass of electrons than that of the holes. We estimate the electron effective mass by assuming single band model. In the nondegenerate case, $S(T)$ is given as

$$S(T) = \pm \frac{k_B}{|e|}\left[\eta - \left(r + \frac{5}{2}\right)\right] \quad (1)$$

with

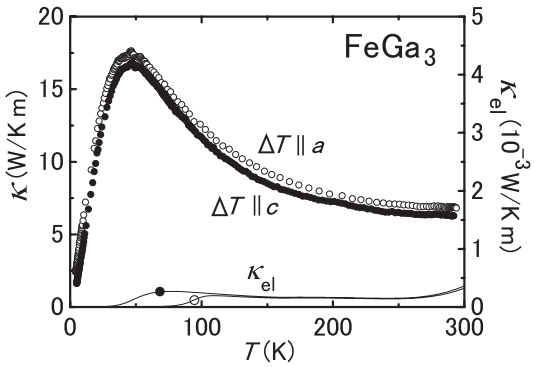

Fig. 5. Temperature dependence of thermal conductivity $\kappa(T)$ along the a- and c-axes of $FeGa_3$. Solid lines are the electronic charge carrier part $\kappa_{el}(T)$ calculated by using the Wiedemann–Franz law $\kappa_{el} = L_0 T/\rho$ from the electrical resistivity.

$$\eta = \ln\left[\frac{n\hbar^3}{2(2\pi m^* k_B T)^{3/2}}\right], \quad (2)$$

where η is the reduced Fermi energy, r is the scattering factor, n is the carrier density, m^* is the electron effective mass, h is Planck's constant, and k_B is Boltzmann's constant.[26] When the carriers are scattered by the thermal vibrations of the lattice, μ is proportional to T^{r-1}. As $\mu \propto T^{-5/2}$ was observed in the range from 100 to 300 K, we obtain r as $-3/2$. Then the above relation between r and S gives the effective mass $m^* = 0.2m_0$ at 300 K, where m_0 is the free electron mass.

Figure 5 shows the temperature dependence of κ measured with the temperature gradient along the a- and c-axes. There is essentially no anisotropy. For intermetallic compounds, κ consists of the electronic charge carrier part κ_{el} and the phonon part κ_{ph}. The $\kappa_{el}(T)$ is in general estimated from the Wiedemann–Franz law $\kappa_{el} = L_0 T/\rho$, where $L_0 = 2.45 \times 10^{-8}\,W\Omega/K^2$ is the Sommerfeld value, and ρ is the measured electrical resistivity. The estimated κ_{el} in our crystals is less than 0.01% of the total κ in the whole temperature range (right axis in Fig. 5). The presence of a peak in $\kappa(T)$ at 50 K is a characteristic of a crystalline solid. It is noteworthy that the maximum value of κ for $FeGa_3$ is much smaller than that of FeSi (15–30 W/Km) and $FeSb_2$ (500 W/Km).[8,14] The small κ is a positive factor for thermoelectric materials.

The temperature dependences of the magnetic susceptibility $\chi = M/B$ and specific heat C for $FeGa_3$ are presented in Figs. 6(a) and 6(b), respectively. The diamagnetic behavior and the weak temperature dependence above 150 K agree with the data reported by Tsujii *et al.*[19] They further found a rapid increase in χ above 500 K, which was interpreted as the thermal excitation of electrons to the conduction band above the gap.[19] The $C(T)$ shown in Fig. 6(b) nearly reaches the Dulong and Petit value of 100 J/(K·mol) at 300 K. The plot of C/T vs T^2 in the inset is linear below 3.5 K and the extrapolation of C/T to $T = 0$ yields the electronic specific-heat coefficient $\gamma = 0.03\,mJ/(K^2 \cdot mol)$. This small value is consistent with the fact that the Fermi level lies in the energy gap, but it is a good contrast to the sizable value of 2–4 mJ/(K^2·mol) reported for FeSi[9] and $FeSb_2$.[13] The appearance of impurity induced states with rather heavy mass at the Fermi

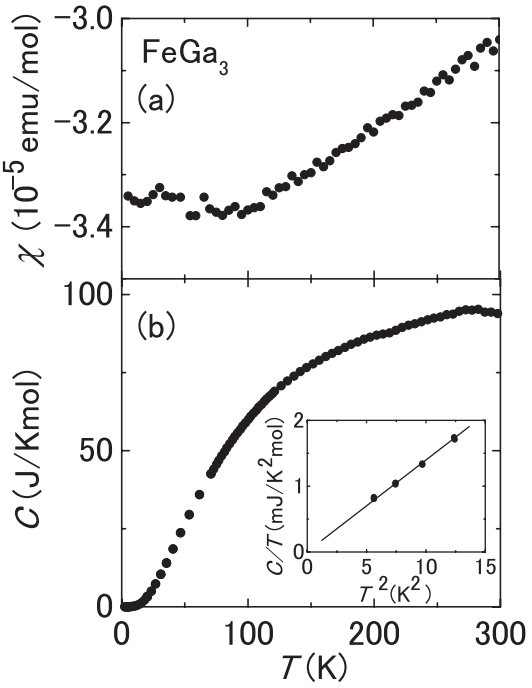

Fig. 6. Temperature dependence of (a) magnetic susceptibility $\chi = M/B$ and (b) specific heat of $FeGa_3$. The inset is a plot of C/T vs T^2.

level is considered to be a characteristic of Kondo semiconductors.[15)]

In conclusion, we have presented thermoelectric and magnetic properties of single crystalline samples of the narrow-gap semiconductor $FeGa_3$. The anisotropy in these properties is very weak despite of the tetragonal crystal structure. The activation behaviors in $\rho(T)$ and career density $n(T)$ in the intrinsic range above 300 K give energy gaps 0.47 and 0.54 eV, respectively, whose values agree with the band gap energy obtained by the band calculations based on local density approximation. The gap value is one order of magnitude larger than that in the Kondo semiconductors FeSi and $FeSb_2$, whose transport gaps are 0.08 and 0.02 eV, respectively.[5,10)] The absence of impurity induced density of states at the Fermi level is indicated by the extremely small γ value of 0.03 mJ/(K^2·mol). These facts suggest that correlation effects or the nature of the Kondo semiconductor in $FeGa_3$ are much weaker than in FeSi and $FeSb_2$. To confirm this point, an optical conductivity study in a wide temperature range is on demand. Interestingly enough, $\rho(T)$ of $FeGa_3$ largely decreases on cooling from 260 to 100 K in the saturation range. This unusual behavior is attributed to the strong temperature dependence of career mobility $\mu \propto T^{-5/2}$. Although the $S(T)$ exhibits a large negative minimum of $-350\,\mu V/K$ at 300 K, the thermoelectric figure of merit $ZT = S^2T/\rho\kappa$ is merely 1.4×10^{-4} at 300 K due to the large value of $\rho = 2\,\Omega$ cm at 300 K. The $\kappa(T)$ exhibits a crystalline peak, whose value is lower by one or two orders of magnitude than those of FeSi and $FeSb_2$. Finally, it should be mentioned that Co substitution for Fe in $FeGa_3$ has enhanced the ZT by more than 10%.[27)] Further enhancement may be possible if a fine tuning of substitution is made on not only the Fe site but also the Ga site in $FeGa_3$.

Acknowledgments

We thank Y. Shibata for performing electron-probe microanalysis and A. Yamamoto for providing valuable information on the thermoelectric properties of $Fe_{1-x}Co_xGa_3$. The authors thank C. Petrovic and T. Kohara for useful discussions. This work was financially supported by a Grant-in-Aid for Scientific Research (A) (No. 18204032) from the Ministry of Education, Culture, Sports, Science and Technology, Japan.

1) D. N. Basov, F. S. Pierce, P. Volkov, S. J. Poon, and T. Timusk: Phys. Rev. Lett. **73** (1994) 1865.
2) Y. Nishio, M. Kato, S. Asano, K. Soda, M. Hayasaki, and U. Mizutani: Phys. Rev. Lett. **79** (1997) 1909.
3) V. Jaccarino, G. K. Wertheim, J. H. Wernick, L. R. Walker, and S. Arajs: Phys. Rev. **160** (1967) 476.
4) Z. Schlesinger, Z. Fisk, H.-T. Zhang, M. B. Maple, J. F. Ditusa, and G. Aeppli: Phys. Rev. Lett. **71** (1993) 1748.
5) D. Mandrus, J. L. Sarrao, A. Migliori, J. D. Thompson, and Z. Fisk: Phys. Rev. B **51** (1995) 4763.
6) S. Paschen, E. Felder, M. A. Chernikov, L. Degiorgi, H. Schwer, H. R. Ott, D. P. Young, J. L. Sarrao, and Z. Fisk: Phys. Rev. B **56** (1997) 12916.
7) T. Saso and K. Urasaki: J. Phys. Chem. Solids **63** (2002) 1475.
8) B. Buschinger, C. Geibel, F. Steglich, D. Mandrus, D. Young, J. L. Sarrao, and Z. Fisk: Physica B **230–232** (1997) 784.
9) S. Yeo, S. Nakatsuji, A. D. Bianchi, P. Schlottmann, Z. Fisk, L. Balicas, P. A. Stampe, and R. J. Kennedy: Phys. Rev. Lett. **91** (2003) 046401.
10) C. Petrovic, J. W. Kim, S. L. Bud'ko, A. I. Goldman, P. C. Canfield, W. Choe, and G. J. Miller: Phys. Rev. B **67** (2003) 155205.
11) C. Petrovic, Y. Lee, T. Vogt, N. Dj. Lazarov, S. L. Bud'ko, and P. C. Canfield: Phys. Rev. B **72** (2005) 045103.
12) A. Perucchi, L. Degiorgi, R. Hu, C. Petrovic, and V. F. Mitrovic: Eur. Phys. J. B **54** (2006) 175.
13) A. Bentien, G. K. H. Madsen, S. Johnsen, and B. B. Iversen: Phys. Rev. B **74** (2006) 205105.
14) A. Bentien, S. Johnsen, G. K. H. Madsen, B. B. Iversen, and F. Steglich: Europhys. Lett. **80** (2007) 17008.
15) T. Takabatake, F. Iga, T. Yoshino, Y. Echizen, K. Katoh, K. Kobayashi, M. Higa, N. Shimizu, Y. Bando, G. Nakamoto, H. Fujii, K. Izawa, T. Suzuki, T. Fujita, M. Sera, M. Hiroi, K. Maezawa, S. Mock, H. v. Löhneysen, A. Bruckl, K. Neumaier, and K. Andres: J. Magn. Magn. Mater. **177–181** (1998) 277.
16) C. Dasarathy and W. Hume-Rothery: Proc. R. Soc. London, Ser. A **286** (1965) 141.
17) U. Häussermann, M. Boström, P. Viklund, Ö. Rapp, and T. Björnängen: J. Solid State Chem. **165** (2002) 94.
18) Y. Imai and A. Watanabe: Intermetallics **14** (2006) 722.
19) N. Tsujii, H. Yamaoka, M. Matsunami, R. Eguchi, Y. Ishida, Y. Senba, H. Ohashi, S. Shin, T. Furubayashi, H. Abe, and H. Kitazawa: J. Phys. Soc. Jpn. **77** (2008) 024705.
20) Y. Amagai, A. Yamamoto, T. Iida, and Y. Takanashi: J. Appl. Phys. **96** (2004) 5644.
21) B. Yates: J. Electron. Control **6** (1959) 26.
22) N. F. Mott and E. A. Davis: *Electronic Processes in Non-crystalline Materials* (Clarendon Press, Oxford, U.K., 1979) 2nd ed., Chap. 2.
23) H. Ibach and H. Lüth: *Solid-State Physics* (Springer-Verlag, Berlin, 1993) p. 290.
24) M. Suzuno, Y. Ugajin, S. Murase, and T. Suemasu: J. Appl. Phys. **102** (2007) 103706.
25) Z. Dashevsky, A. Belenchuk, E. Gartstein, and O. Shapoval: Thin Solid Films **461** (2004) 256.
26) G. S. Nolas, J. Sharp, and H. J. Goldsmid: *Thermoelectrics Basic Principles and New Materials Developments* (Springer, New York, 2001) p. 41.
27) Y. Amagai, A. Yamamoto, T. Iida, and Y. Takanashi: Proc. 23rd Int. Conf. Thermoelectrics, 2005, p. 116.